Exergoeconomic and multi-objective optimization of a solar system for Hydrogen production by the Particle Swarm Algorithm

Ehsanolah Assareh[1,2*] ,Sajjad Keykhah[1],Ali Heidary Moghadam[2], Reza Poultangari[1,2], Tahereh Pirhoushyaran[3]

[1]Department of Mechanical Engineering, Dezful Branch, Islamic Azad University, Dezful, Iran
[2]Materials and Energy Research Center, Dezful Branch, Islamic Azad University, Dezful, Iran
[3]Department of Chemical Engineering, Dezful Branch,Islamic Azad University,Dezful,Iran

Resceived: Spring 2019 Accepted: Spring 2019

Abstract

Due to the rapid depletion of fossil energy resources and the environmental pollutions caused by consumption of fossil fuels, many countries have started developing renewable energy systems and finding alternative energy resources. One of the best resources of renewable energy is solar energy, which is clean and carbon-free. Solar-based energy systems can be designed in a way to produce hydrogen energy in order to supply the global energy demand, and reducing the environmental effects caused by global warming. In this study, a solar-based integrated hybrid system is considered to generate hydrogen. The system takes advantage of a flat plate collector, an organic Rankine cycle (ORC) and a PEM electrolyzer to convert renewable solar energy into electricity and hydrolyze water to hydrogen gas. To determine the optimum parameters and evaluate their effects on performance of the system, a parametric study is conducted. Outlet temperature of generator, inlet temperature of ORC turbine, irradiation intensity, water mass flow rate of the collector, and collector surface area are considered as the five decision variables. To optimize the design parameters, a multi-objective optimization is performed through the multi-objective particle swarm algorithm. The optimization results indicate that exergy efficiency of the system can increase from 1 to 3.5% meanwhile the total cost of the system can increase from 21 to 28 $/h, at optimum conditions. According to the findings, extending the collector's surface area can lead to increasing the overall cost of the system, whilst reducing the exergy efficiency. It can also be stated that the collector component contributes to the total cost of the system noticeably.

***corresponding author: assareh@iaud.ac.ir,**

Keywords: Solar energy, hydrogen generation, optimization, flat plate collector, exergy efficiency, cost rate.

[DOR: 20.1001.1.20089813.1398.6.1.6.6]

1. Introduction

Fast growth of energy demand, increase of global warming and greenhouse effects has attracted a growing attention towards renewable sources of energy. One of the most common and viable renewable sources is solar energy, which is easily accessible and cheap while providing noticeable power. Moreover, solar energy can be used in many ways and it can be converted to the other types of energy. This natural source of power has been widely used around the universe since it is abundant and endless and it does not require costly and huge networks to be transferred and distributed. Nowadays, different technologies have been developed to utilize solar energy including solar collectors, which generate thermal energy and photovoltaic panels producing electricity. In recent years, one of the main challenges related to solar energy has been to generate different sorts of energy from solar radiations without releasing greenhouse gases. Also, it has been attempted to design a system with high efficiency and low cost, as one of the most important objectives in the field of energy systems. One of the promising technologies for this purpose refers to flat plate solar collectors (FPSCs), which can be designed simply and fabricated conveniently. Since 1980s, various types of solar collectors have been used to develop different energy systems, such as solar panels, parabolic trough and solar towers. A FPSC can provide warm water with a temperature lower than 100 °C to feed other energy systems. Though many studies have evaluated solar energy systems to supply various outputs, few researchers have attempted to perform multi-objective optimization (MOO) of renewable energy systems for hydrogen production. As a matter of fact, Hydrogen is an energy source that can prevent environmental pollutions and the disadvantages of using fossil fuels. Its energy efficiency is higher than the energy efficiency of fossil fuels. Hydrogen can be produced by using a variety of energy resources and used in all applications of fossil fuels. In the following parts, a review of recent studies concerning the Hydrogen production using the renewable sources of power are presented and discussed.

Ahmadi et al. [1] studied application of ocean energy to generate hydrogen. They showed that the energy and exergy efficiencies of their developed hybrid system are 3.6% and 22.7%, respectively. They also concluded that it is possible to produce 1.2 kg h^{-1} hydrogen using the power generated by the devised organic Rankine cycle (ORC). Bichar et al. [2] devised a new hybrid system that consumes solar and geothermal energies to generate hydrogen. The two employed types of energy can boost each other, prevent reduction of the system's efficiency in the absence of one of the two resources and enhance efficiency of the overall system. Their devised system is consisted of an ORC, a thermal pump, an absorption chiller system, a thermal energy reservoir and a hydrogen generator system. Ahmadi et al. [3] designed a new multifunction energy system to generate power, hydrogen and fresh water based on solar energy. They concluded that the exergy efficiency of their hybrid system is 60% and the total cost rate is 154 \$ h^{-1}, at optimum conditions. Joshi et al. [4] investigated the effects of various parameters on a hydrogen generator solar system. They considered a solar energy-based hydrogen generation system and the two objectives of energy and exergy. They concerned the variable parameters of solar irradiation intensity (I), environmental temperature (T), heat transport (heat coefficient; q) and the absorbent's surface area (A). Yuksel et al. [5] analyzed a geothermal energy based integrated system, which was designed to generate electricity and provide drinking water, heat and cooling. Their system uses geothermal energy for its ORC and absorption chiller system and produces hydrogen using an electrolyzer.

A portion of the electricity current generated by the ORC supplies the energy needed for the electrolyzer. Also, the heat obtained from geothermal resources can preheat the inlet water of the electrolyzing process. Ahmadi et al. [6] performed a multi-objective optimization process for an energy system that relies on ocean energy for hydrogen production. Ocean thermal energy conversion (OTEC) systems typically contain a low-temperature ORC that warms and evaporates the working fluid, i.e. ammonia, and the produced vapor satisfies the turbine's requirement for electricity generation. In their optimization process, Ahmadi et al. evaluated the two opposite objectives of cost and exergy through an evolutionary algorithm and minimized the total cost of the system meanwhile optimizing exergy utilization.Ahmadi et al. [7] worked on MOO of a new multifunctional solar energy based system. Their case system relies an ocean energy conversion and is equipped with a flat plate solar collector, a reverse osmosis based desalination unit for providing fresh water, a single-effect absorption chiller and a PEM electrolyzer. The system was studied thermodynamically. They determined the optimum design parameters according to a smart non-dominative sorting genetic algorithm (NSGA-11). In their optimization, the two objective functions were the total cost rate of the system including the costs associated

[DOR: 20.1001.1.20089813.1398.6.1.6.6]

with energy, fuel, purchasing the system components and environmental impacts, and the exergy efficiency of the cycle, which was maximized by an evolutionary algorithm. .Dincer and Zamfirsco [8] analyzed the energy and exergy of a multifunctional system that was based on renewable energy resources. They considered different production options, such as electricity, heat, hot water, cooling, hydrogen and fresh water. Ozturk and Dincer [9] carried out a thermodynamics analysis on a solar energy based multifunctional system that could produce hydrogen. The outputs of the system included power, heating, cooling, warm water, hydrogen and oxygen. Their studied system was composed of a Rankine cycle, an ORC, an absorption chiller and heater and a hydrogen generation unit. Their obtained values of efficiency and exergy loss for the subsystems and the general system showed that the highest exergy loss is related to the parabolic dish collectors.Al Soleyman et al. [10], in 2013, studied the three multifunctional systems of solid oxide solar cells, biomass and mobile solar system. Their investigations revealed that the multifunctional mobile solar system has the best thermoeconomic performance due to presenting the lowest cost per unit exergy, compared with the two other systems. Yilmaz et al. [11], in 2012, focused on a system working with geothermal energy and containing an electrolyzer for hydrogen production. They performed seven different types of modeling and concluded that increased temperature of the geothermal resource can reduce the costs of production and hydrogen liquefaction.Owali et al. [12] used geothermal energy of the geothermal regions of Aljazeera to utilize hydrogen sulfide for hydrogen generation. They evaluated various aspects of this issue.Yuksel et al. [13] introduced a new multifunctional hybrid system based on solar energy to produce power, hydrogen, warm water, cooling and heat, simultaneously. They stated that the temperature of the interior parts of the absorption tubes and intensity of solar irradiation have a direct relationship with the extent of hydrogen generation. The method of swarm particles optimization is a social search algorithm that is inspired from the nature. When a group is moving towards a predefined object, any member in the swarm tries to modify its route according to the best known position in its memory and the best position identified in its social cycle and the member records the best path in its memory. In the current paper, we aim to investigate and optimize a solar energy system for the purpose of hydrogen production. In addition, an integrated system containing a FPSC, an ORC, a PEM electrolyzer and a single-effect absorption chiller is evaluated thermodynamically and optimized by a multi-objective particle swarm algorithm (MOPSA), for the first time.

In next part of the study, the efficiency and the total cost of the system are calculated, in addition to calculating the amounts of the generated hydrogen and electricity. Furthermore, a parametric study is performed to determine the parameters that are effective on the performance of the system. In order to optimize the system, the MOPSO is applied to the two objectives of exergy efficiency and the total cost, which should be maximized and minimized, respectively. The optimization algorithm is validated based on the analysis performed by Khanmohammadi et al. [27].

2. Description of the proposed system

Fig. 1 depicts the schematic of the integrated system proposed for hydrogen production. This system is consisted of four main subsystems: an ORC, a PEM electrolyzer, a single-effect absorption chiller and a FPSC. The working fluid of the ORC is R134a.In order to produce hydrogen, the electrolyzer is coupled with the other components of the system. The energy required for operating the system and the ORC is supplied by solar energy. Therefore, there is no need for using the fossil fuels to provide the ORC with energy and therefore no environmental contaminant would be produced. Hydrogen production relies on transferring the power generated by the ORC to the electrolyzer. Performance and the parameters of the designed hybrid system at their initial statuses are reported in Table 1. Table 2 presents the principal variables of the optimization process.

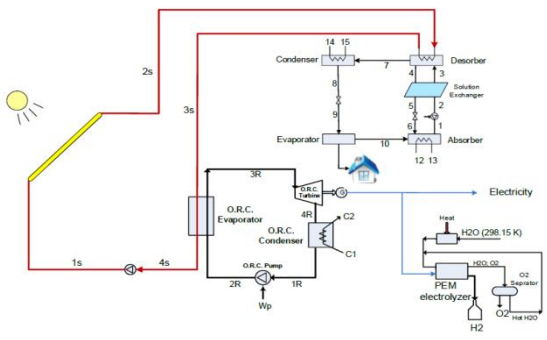

Fig. 1. Schematic diagram of the integrated hybrid system accompanied with a FPSC.

[DOR: 20.1001.1.20089813.1398.6.1.6.6]

Table 1. Operational properties of the system.

Parameter	Value	Unit
Surface area of the FPSC	4000	m^2
Inlet temperature of the collector	27	°C
Water mass flow of the collector	5	kg/s
Irradiation intensity per unit surface area of the flat plate collector (I)	500	w/m^2
Optical efficiency: $\eta=\mathcal{T}\alpha$	0.84	-
Maximum inlet temperature of the ORC turbine (T_{3R})	50	°C
Temperature of the inlet water of the ORC operator	55	°C
Electricity ratio of the ORC outlet to the PEM inlet	0.5	(-)

Table 2. The main parameters considered during the optimization process of the system.

Unit	Parameter	Variable
°C	T_{3R}	ORC turbine inlet temperature
°C	T_{3S}	Generator (or Evaporator?) outlet temperature
m^2	A_p	Flat plate collector area
Kg /s	$\dot{m}_{co}$	Collector water mass flow rate
w/ m^2	I	Irradiation intensity

3. Thermodynamics modeling

Each component of the hybrid system can be considered as a control volume at steady state condition. Then, the corresponding equations can be derived. The forthcoming subsections describe derivation of the required equations:

3.1. The Flat Plate Solar Collector

As shown in Fig. 1, the water flow entering the solar collector warms at point 1s. When temperature of the flow reaches T_{2s}, its energy increases. The heat obtained from the working fluid can be written as:

$$\dot{Q}_u = \dot{m}_{col} C_p (T_{2s} - T_{1s}) \qquad (1)$$

ere, T_{2s} is the temperature of the outlet water, T_{1s} refers to the temperature of the inlet water, C_p is specific heat at constant pressure and $\dot{m}_{col}$ is the collector's water mass flow rate. The heat obtained from the FPSC can be calculated through the hotelier equation [41] by considering the collector's heat loss:

$$\dot{Q}_u = A_P F_R [(\tau\alpha) I - \mathrm{Q}_L) \qquad (2)$$

ere, F_R is the factor of heat loss and can be defined as the Eq. 3, in which F' is the factor of collector efficiency (≈0.914) and U_l is the coefficient of the collector's total loss that is calculated in Ref. [14].

$$F_R = \frac{\dot{m}_{col} C_p}{U_l A_P} \left[1 - e^{\{-\frac{F U_l A_P}{\dot{m}_{col} C_p}\}} \right] \qquad (3)$$

In Eq. 2, $\tau\alpha$ is the visual efficiency and I is intensity of solar irradiation while Q_L can be determined through Eq. 4 at room temperature (T_0). The energy efficiency of the FPSC can be stated as [14]:

$$Q_L = U_l (T_{in} - T_\circ) \qquad (4)$$

$$\eta = \frac{\dot{Q}_u}{I\, A_P} \qquad (5)$$

3.2. The ORC

As shown in the schematic system (Fig. 1), warm water enters the ORC's evaporator at point 3S and transfers its heat to the working fluid of the ORC. The equations that rule the ORC at steady state can be summarized according to the Eq. 6 [28]:

$$\dot{m}_{col}(h_{3s} - h_{4s}) = \dot{m}_{2R} h_{2R} - \dot{m}_{3R} h_{3R} \qquad (6)$$

where h_{3S}, h_{4S}, h_{2R} and h_{3R} are enthalpies of the inlet of the ORC's evaporator (the water side), the fluid inlet to the collector's pump, inlet of the ORC's evaporator (the ORCs working fluid side) and outlet of the ORC's evaporator (the ORCs working fluid side), respectively.

At the ORC's turbine:

$$\dot{W}_T = \dot{m}_{3R}(h_{3R} - h_{4R}) \qquad (7)$$

At the ORC's condenser:

$$\dot{m}_{cooling\ water}\left(h_{out;cooling} - h_{in;cooling}\right) = \dot{m}_{1R}(h_{1R} - h_{4R}) \qquad (8)$$

At the ORC's pump:

$$\eta_{is,pump} = \frac{h_{2Rs} - h_{1R}}{h_{2R} - h_{1R}} \qquad (9)$$

Where, $\eta_{is,pump}$ is related to the efficiency of the isentropic pump.

3.3. The PEM electrolyzer

In the current study, hydrogen is used as an energy carrier and the main goal is generating hydrogen. For this purpose, a PEM electrolyzer is added to the proposed system. It means that the electrolyzer is

[DOR: 20.1001.1.20089813.1398.6.1.6.6]

meant to produce hydrogen gas. The employed PEM electrolyzer is illustrated in Fig 1. The electrolyzer consumes the electricity current generated by the ORC to hydrolyze water. The required liquid water enters the electrolyzer at room temperature. Afterwards, in the thermal convertor, the water is heated up to the PEM's temperature electrolyzer, i.e. about 363 K. After heating, the water is directed from the heat convertor to the electrolyzer to produce hydrogen and oxygen at the cathode and the anode, respectively. The generated hydrogen gas diffuses out of the water and oxygen mixture and cools down to room temperature. Then, the remained water recirculates for hydrogen production. The generated hydrogen would be stored in a reservoir for further applications. It should be noted that the related reaction is simply a water hydrolysis process, which means that the electricity and heat are used to dissociate water into hydrogen and oxygen.

3.4. Absorption chiller

In each absorption chiller, a fluid acts as the absorption fluid while the other fluid acts as the chiller. Here, a solution of lithium bromide is used as the absorption fluid and water flows as the chiller fluid. The principles of mass conversion and the first and the second laws of thermodynamics should be applied to each component of the single-effect absorption chiller. The equations that describe total mass and the mass of each solution at steady state for laminar flows can be written as follows [16]:

$$\sum \dot{m}_{in} = \sum \dot{m}_{out} \quad (10)$$

$$\sum (\dot{m}x)_{in} = \sum (\dot{m}x)_{out} \quad (11)$$

Where, $\dot{m}$ is the mass flow rate of the working fluid and x is the weight percentage of LiBr in the solution. For each component of the absorption system, the general energy balance can be formulated as:

$$\dot{Q} - \dot{W} = \sum \dot{m}_{out}\, h_{out} - \sum \dot{m}_{in}\, h_{in} \quad (12)$$

Also, the chiller's capacity of absorption can be defined by:

$$\dot{Q}_{in} = \dot{m}_9(h_{10} - h_9) \quad (13)$$

Ref. 17 provides more details about the thermodynamics modeling and energy balance of each component.

3.5. Exergy analysis

Exergy is defined as the maximum useful work that can be obtained from a system or material flow during the process of system equilibration with its environment [18]. In the absence of nuclei changes, magnetic field, electricity effects and surface tension, each term of exergy can be divided into four main parts. These four parts include physical exergy, chemical exergy, potential exergy and kinetic exergy. Eq. 14 shows the resultant exergy relationship.

$$ex = ex_{ch} + ex_{ph} + ex_{pt} + ex_{kn} \quad (14)$$

If the changes in velocity and height are negligible, the potential and kinetic exergy contributions can be ignored. Physical exergy depends on pressure and temperature, considerably. In order to estimate the physical exergy, the following equation can be employed:

$$ex_{ph} = (h - h_\circ) - T_\circ(s - s_\circ) \quad (15)$$

$$ex_{ch} = \sum \mathrm{x}_k ex^k{}_{ch} + RT_\circ \sum \mathrm{x}_k \ln(\mathrm{x}_k) \quad (16)$$

Where the ° subscript indicates standard conditions. Chemical exergy is equal to the maximum work [18]. Chemical exergy of a gas mixture can be written as:

$$\dot{ex}_{H_2} = \dot{m}_{H_2}(ex_{ph} + ex_{ch})_{H_2} \quad (17)$$

Exergy of hydrogen gas (H_2) follows Eq. 17, in which $\dot{m}_{H_2}$ refers to the mass flow rate of hydrogen (kg s^{-1}). Physical exergy can be considered as the maximum useful work that can be theoretically calculated for a system interacting with its environment at equilibrium conditions. The physical exergy of hydrogen can be calculated according to Eq. 15 while its chemical exergy (ex_{ch}) is:

$$\mathrm{ex_{ch}} = \frac{253153}{M_{H_2}} \quad (18)$$

$$\dot{E}x_Q + \sum \dot{m}_{in}\mathrm{ex_{in}} = \sum \dot{m}_{out}\mathrm{ex_{out}} + \dot{E}X_W + \dot{E}X_D \quad (19)$$

Where ex_{ch} is the molar mass of hydrogen (kg $kmol^{-1}$). The following equation can be derived for exergy balance based on the first and the second laws of thermodynamics, in which $\dot{E}x_Q$, $\dot{\mathrm{E}}\mathrm{x}_\mathrm{W}$ and $\dot{E}x_D$ correspond to the status of heat exergy, the rate of work exergy and the rate of exergy loss, respectively [21]:

3.6. Economic analysis

[DOR: 20.1001.1.20089813.1398.6.1.6.6]

The main objective of economic modeling is derivation of a function for the rate of total costs of the system. There are different methods for determining the purchase cost of equipment based on the design parameters. Bizhan and Moran [20] introduced several useful functions for calculating the purchase cost of equipment in a thermal system. Their recommended functions can estimate the main equipment costs by considering the size of the elements, effectively. Table 3 presents the cost functions of each hybrid system component based on the design parameters.

Table 3. Cost functions for each system component [1,23,14].

Components	Cost functions
ORC evaporator	$Z_{ev} = 309.14(A_{ev})^{0.88}$
ORC pump	$Z_{pump} = 200(\dot{W}_{pump})^{0.65}$
ORC turbine	$Z_{tur} = 4750(\dot{W}_{tur})^{0.6}$
ORC turbine	$Z_{cond} = 516.62(A_{cond})^{0.6}$
Absorption chiller	$Z_{chiller} = 1144.3(\dot{Q}_{ev})^{0.67}$
Flat plate collector	$Z_{flatplate} = 235(A_{flatplate})$
Proton exchange membrane (PEM) electrolyzer	$Z_{PEM} = 1000\dot{W}_{PEM}$

Since each piece of the system is expected to work in a definite time framework, the cost rate of each piece is a proper measure of cost calculation. Cost rate of each piece ($\dot{E}x_D$; \$/h) can be determined using [15]:

$$\dot{Z}_K = \frac{Z_k \times CRF \times \varphi}{N \times 3600} \qquad (20)$$

Here, Z_k is the purchase cost of the k*th* piece and CRF is the capital return factor. N is the annual operational time (h) for the unit and φ refers to the maintenance parameter, which is usually equal to 1.06 [25].

$$\psi = \frac{\dot{m}_{H_2} Ex_{H_2} + \dot{E}x_{cooling} + \dot{E}x_{electricity}}{\dot{E}x_{in;collector}} \qquad (21)$$

3.7. Optimization

To assess the system precisely and evaluate the effect of the design parameters on the thermodynamic and economic performance of the system, exergy efficiency and total cost rate were concerned as two opposing objective functions, which should be respectively maximized and minimized. The objective function of exergy efficiency can be defined as Eq. 21. In this equation, ψ stands for exergy efficiency of the system and $\dot{E}x_{in,collector}$ is the rate of exergy input to the collector through solar energy.

$$\dot{E}x_{in;collector} = \eta_\circ I\, A_p \left(1 - \frac{T_\circ}{T_{sun}}\right) \qquad (22)$$

By using a useful relationship and considering solar energy as an unlimited thermal resource, the rate of exergy input to the solar collector can be calculated through Eq. 22, in which T_{sun} is the apparent temperature of the sun that is equal to 75% of its dark body [30]. Additionally, $\dot{E}x_{electricity}$ refers to the outlet electrical exergy of the system that is equivalent to the portion of electricity fed to external users, such as the PEM electrolyzer. The exergy of cooling ($\dot{E}x_{cooling}$) can be calculated according to the cooling capacity as:

$$\dot{E}x_{cooling} = \dot{Q}_{ev} \left(1 - \frac{T_\circ}{T_{sun}}\right) \qquad (23)$$

$$\dot{C}_{total} = \dot{Z}_{flatplate} + \dot{Z}_{PEM} + \dot{Z}_{PUMP;R} + \dot{Z}_{ev;R} + \dot{Z}_{tur;R} + \dot{Z}_{cond;R} + \dot{Z}_{chiller} \qquad (24)$$

Ex_{H_2} is hydrogen exergy per unit mass that is equivalent to 11.050 kJ kg^{-1} [18]. The secondary objective function, i.e. rate cost, can be written with respect to the rate costs of the system pieces as Eq. 24. Using the MOPSO algorithm and the two objective functions of exergy efficiency and total cost rate, the hybrid system is optimized. The decision making variables are selected by considering the parameters of the system and their impacts on the objective functions. In this way, five variables that affect performance of the system are concerned as the decision variables. These variables include the maximum temperature of the ORC (T_{3R}), the inlet temperature of the ORC's evaporator (T_{3s}), total surface area of the flat plate collector (A_p), mass flow rate of the collector ($\dot{m}_{col}$) and intensity of solar irradiation (I). The upper and lower bounds (the acceptable ranges) of each variable are listed in Table 4. The MOO process was conducted with respect to the variable ranges. Also, the thermodynamics properties of several system points are reported in Table 5.According to the obtained Pareto chart (Fig. 15), the optimum values of exergy efficiency and the total cost rate of the system change from 1 to 3.5% and 21 to 28 \$/h, respectively. To find an optimum relationship between exergy efficiency and the total cost rate of the system, an equation can be

[DOR: 20.1001.1.20089813.1398.6.1.6.6]

fitted into the points obtained through MOO and the corresponding Pareto chart. The fitted equation is:

$$\dot{C}_{total}(\psi) = -0.095143\,\psi^4 + 0.77286\psi^3 - 2.0828\psi^2 + 4.7755\,\psi + 17.8559 \quad (25)$$

It should be noted that the outlined equation is just valid for 1 to 3.5% exergy efficiency and the case system investigated in this research

Table 4. The decision variables and their acceptable ranges.

Decision variables	Lower bound	Upper bound	Limitation
ORC turbine inlet temperature (T_{3R})	$44°C$	$54°C$	Thermodynamic Limitation
Generator outlet temperature (T_{3s})	$55\ °C$	$65\ °C$	Thermodynamic Limitation
Flat plate collector area (A_P)	$٣٠٠٠m^2$	$8000\ m^2$	Commercial limitation
Collector water mass flow rate ($\dot{m}_{col}$)	٢kg/s	٢kg/s	Technical limitation
Irradiation intensity (I)	٣٠٠w/m^2	٢٠٠w/m^2	Environmental Limitation

Table 5. The thermodynamics properties of different points of the hybrid system.

Point	m ($\frac{Kg}{s}$)	P (kPa)	T (°C)	h ($\frac{kj}{kg}$)	s ($\frac{kj}{kgK}$)	Ex (kW)
1s	5	200	27	113.3	0.39	0.17
2s	5	180	75.42	315.8	1.02	16.91
3s	5	180	55	230.4	0.77	6.488
4s	5	180	26.5	111.2	0.39	0.129
1R	2.687	96.49	26.5	227.7	1.1	0.018
2R	2.687	217.1	26.8	228.1	1.1	0.1
3R	2.687	212.7	50	413.2	1.67	14.32
4R	2.687	98.46	27	401.5	1.68	1.885
1	8.693	0.68	34.6	93.1	0.2	1.783
2	8.693	7.42	34.6	97.2	0.2	5.907
3	8.693	7.42	67.6	159	0.4	8.758
4	8.614	7.42	80	185.6	0.47	12.49
5	8.614	7.42	45.62	123.2	0.26	9.463
6	8.614	0.68	35.6	123.2	0.2	27.61
7	0.079	7.42	80	2649.3	8.48	167.3
8	0.079	7.42	40.1	168	0.57	2.708
9	0.079	0.68	1.5	168	0.61	8.383-
10	0.079	0.68	1.5	2503.3	9.11	164.400-
11	8.693	0.68	34.6	93.1	0.2	1.783
12	7.187	100	20	83.9	0.3	0
13	7.187	100	35	146.7	0.5	1.584
14	4.703	100	20	83.9	0.3	0
15	4.703	100	30	125.8	0.44	0.719

4. Results and discussion

4.1. Validation

In order to ensure the accuracy of the optimization algorithm and the programmed code, the MOO results were compared with the results of Khanmohammadi et al. [27]. The corresponding results are presented in Table 6. According to Table 6, at identical conditions, the output results of the objective functions are consistent with the results addressed by [27]. Therefore, the programmed MOO algorithm is valid and reliable. To validate the exergy-economy analysis algorithm more precisely, the effects of any changes in the collector's fluid mass flow rate and the inlet temperature of the ORC's turbine on the two objective functions were compared with the work of [27]. Figs. 2 to 5 exhibit the comparison results.

4.2. Optimum results

In this section, the analysis results of the system are presented and discussed based on the defined objective functions and the results optimized by MOPSA, which comprises the main part of this research. Table 6 reports the thermodynamics modeling results of the system.

[DOR: 20.1001.1.20089813.1398.6.1.6.6]

Table 8. The average values resulted from the optimization analysis.

Parameter	the amount of
Elecrtricity output	24.671 kW
Cooling capacity	49.167 kW
Hydrogen production rate	0.2431 kg/s
Total exergy efficiency	2.2712 %
Total cost rate	21.9462 $/h

Table 9. Average results of the optimized five main variables.

Parameter	Optimum amount
T_{3R}	45.79249 °C
T_{3S}	57.8739 °C
A_p	3000.05741 m^2
m_{col}	5.58549 kg/s
I	400 W/m^2

Table 10. Average properties of the points selected on the Pareto curve.

Point	A	B	C
T_{3R} (°C)	44.4459	46.9086	54
T_{3S} (°C)	58.9993	60.2709	58.393
A_p (m^2)	3002.98	3006.35	3006.13
m_{col} (kg/s)	3.08596	5.43495	5.99857
I (W/m^2)	440	400	400

[DOR: 20.1001.1.20089813.1398.6.1.6.6]

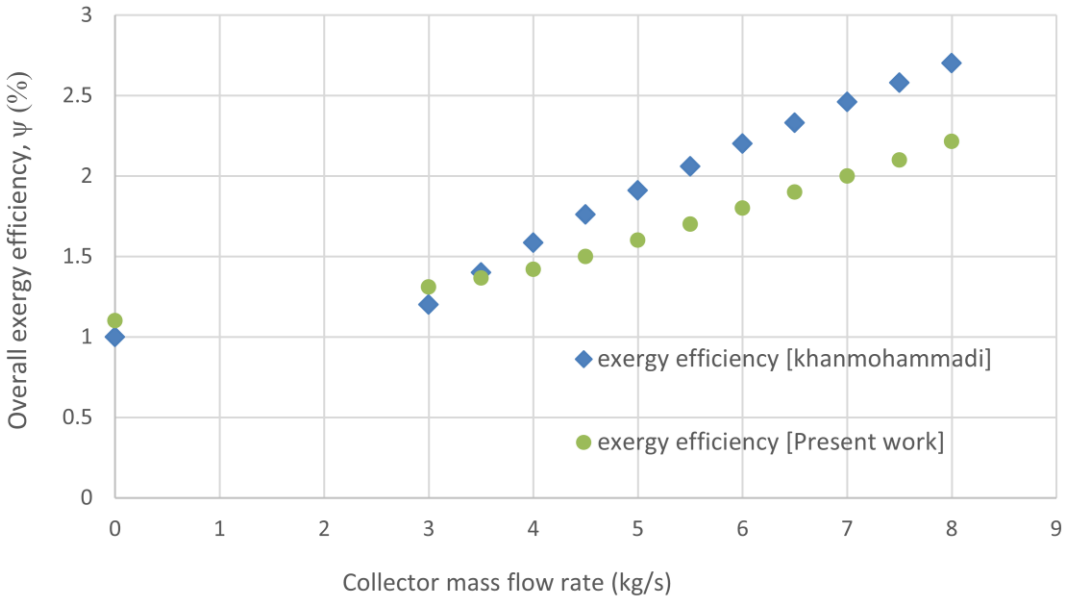

Figure 2. Comparison of the effect of the collector's water mass flow rate on exergy efficiency

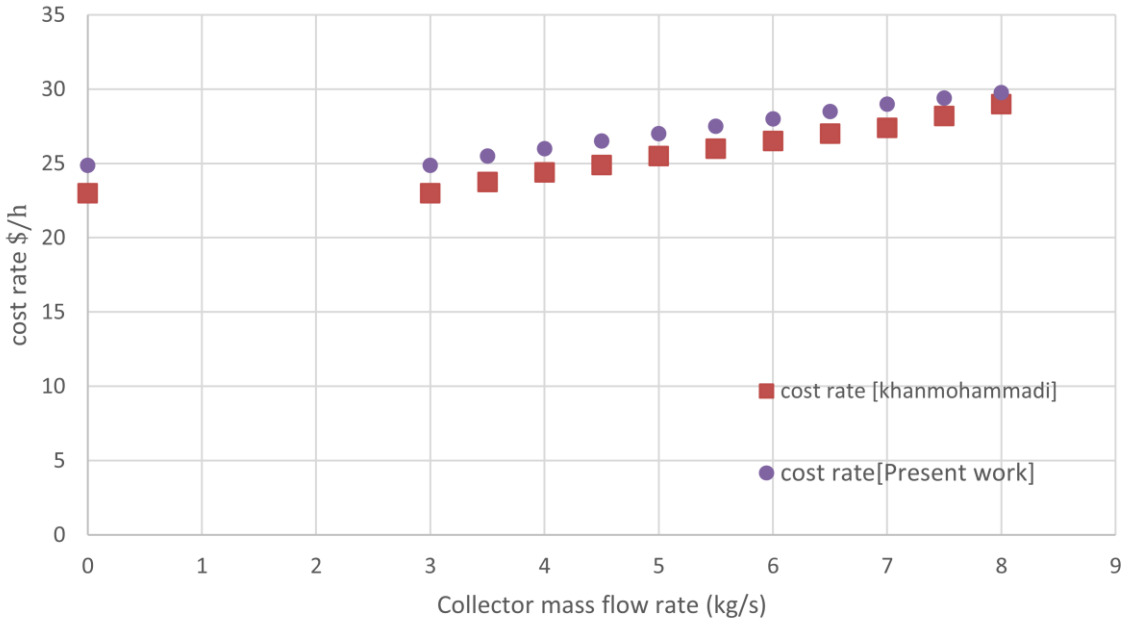

Figure 3. Comparison of the effect of the collector's water mass flow rate on cost rate

[DOR: 20.1001.1.20089813.1398.6.1.6.6]

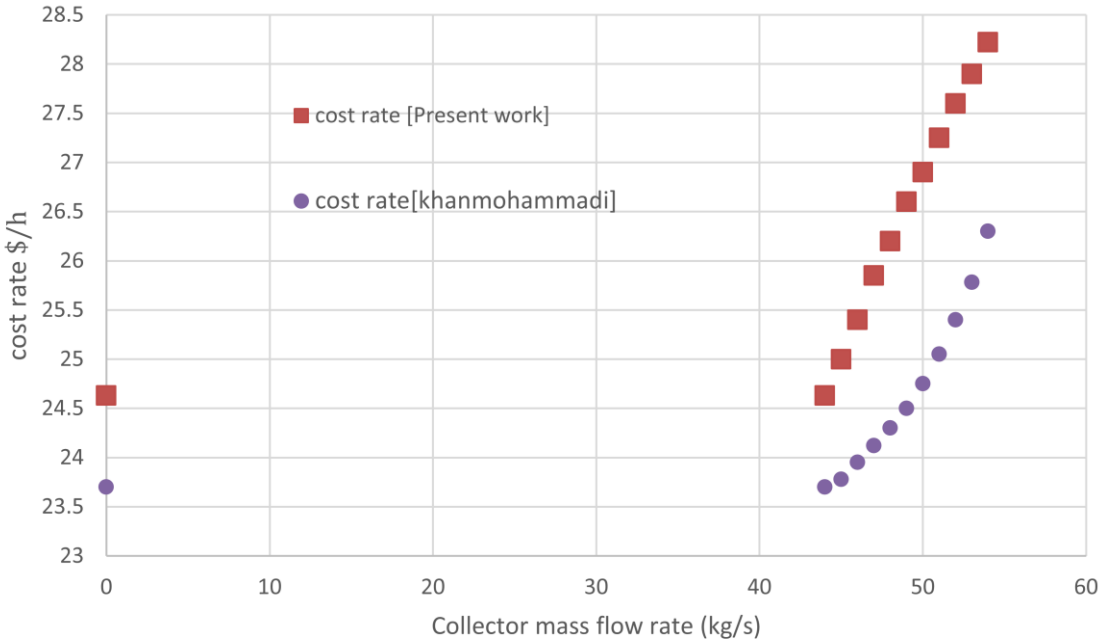

Figure 5. Comparison of the effect of the inlet temperature of the ORC's turbine on cost rate

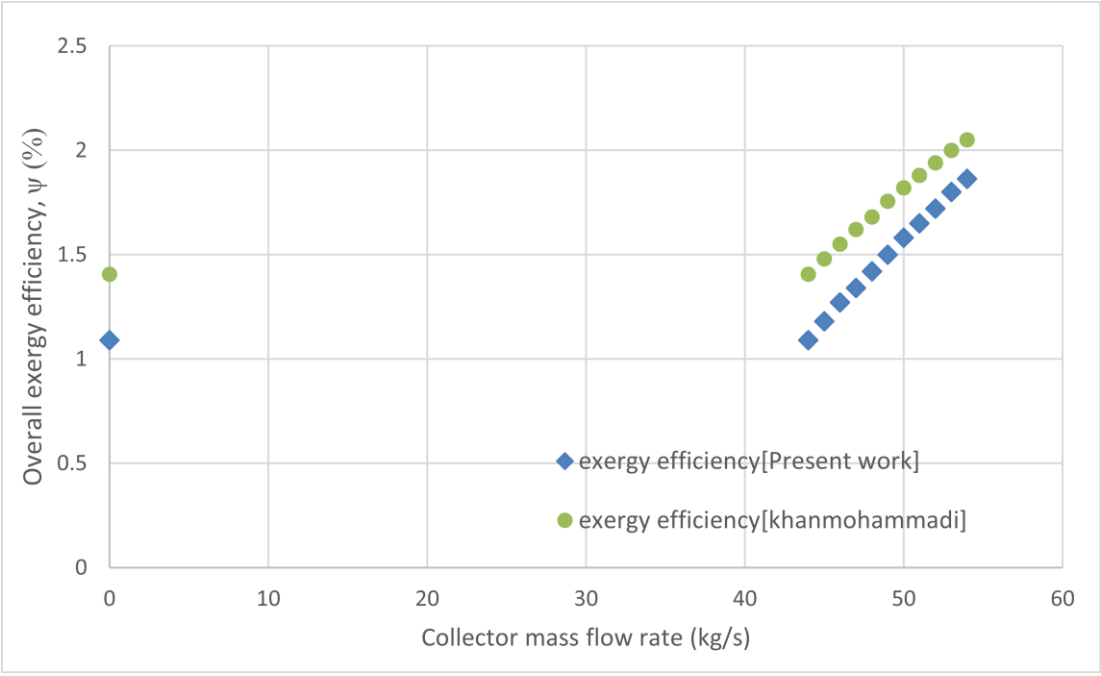

Figure 4. Comparison of the effect of the inlet temperature of the ORC's turbine on exergy efficiency

[DOR: 20.1001.1.20089813.1398.6.1.6.6]

Table 7. The MOO results of the 10 code runs

Parameter	the level 1	the level 2	the level 3	the level 4	the level 5	the level 6	the level 7	the level 8	the level 9	the level 10
Elecrtricity output (kw)	28.1096	18.4602	25.2787	27.3849	28.8361	27.8608	19.8335	25.8738	24.1569	20.9156
Cooling capacity (kw)	49.167	49.167	49.167	49.167	49.167	49.167	49.167	49.167	49.167	49.167
Hydrogen production rate (kg/s)	0.30496	0.13162	0.25411	0.29194	0.31801	0.30049	0.15629	0.2648	0.23395	0.17573
Total exergy efficiency (%)	2.6452	1.596	2.3374	2.5664	2.7242	2.6181	1.7453	2.4021	2.215	1.863
Total cost rate ($/h)	25.4997	22.678	24.6341	25.2873	25.7256	25.4223	23.0595	24.8164	24.2666	23.3601

The principal goal of an exergy-economy analysis is determining the trends of costs and calculating the costs for each unit of exergy produced by a system. The system per exergy unit costs of the products can be used to optimize the economy of the utilized cycle. In this research, to achieve the exact conditions of multi-objective solutions, the code programmed in MATLAB was executed 10 times. Then, the averages of the results were used to analyze and optimize the hybrid system. The results of the runs and the average values are reported in Tables 7 and 8, respectively.As it can be seen in Table 8, the average exergy efficiency of the system is 2.2712%, which is a relatively low efficiency compared with efficiencies of other energy systems. The reason is that this system converts high temperature solar energy to another form of energy at a relatively lower temperature. Therefore, a great portion of exergy loss can be attributed to this energy

conversion process. The optimized values obtained for the five main variables after executing the code 10 times are tabulated in Table 9. Also, the

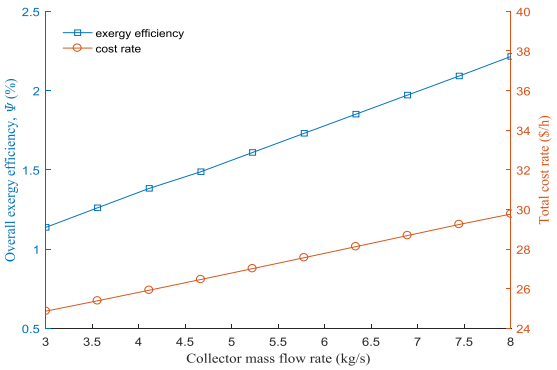

Fig. 6. Variations of the two objective functions with mass flow rate of the collector's water.

Fig. 7 depicts the changes in different system outputs with variation of the collector's water mass flow rate. It can be inferred that increase of the flow rate promotes the rates of hydrogen and electricity generation while it has no significant influence on increasing cooling capacity.

[DOR: 20.1001.1.20089813.1398.6.1.6.6]

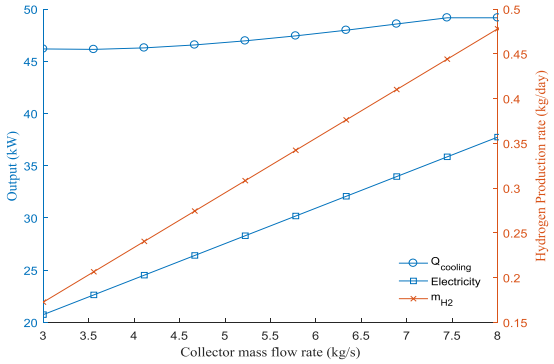

Fig. 7. Changes in the main outputs of the system with the collector's water mass flow rate.

The effect of the inlet temperature of the ORC's turbine, as one of the decision variables, on the objective functions are shown in Fig. 8. Based on this figure, exergy efficiency is enhanced from 1.1 to 2.1%. However, the other objective, i.e. total cost rate, is increased from 25 to 28.2 $/h. This unraveled feature is a very important outcome of MOO, which can optimize both objective functions and determine the best point between their resultant values. The main objectives of this research are increasing exergy efficiency and reducing the total cost of the system.

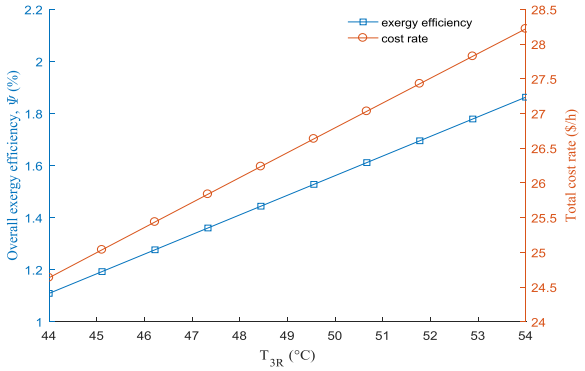

Fig. 8. Effect of the inlet temperature of the ORC's turbine on the objective functions.

Furthermore, the results demonstrate that cooling capacity is not sensitive to T_{3R}. According to Fig. 9, increase of T_{3R} has a positive impact on the rates of hydrogen and electricity generation by the system while it has an insignificant effect on cooling capacity.

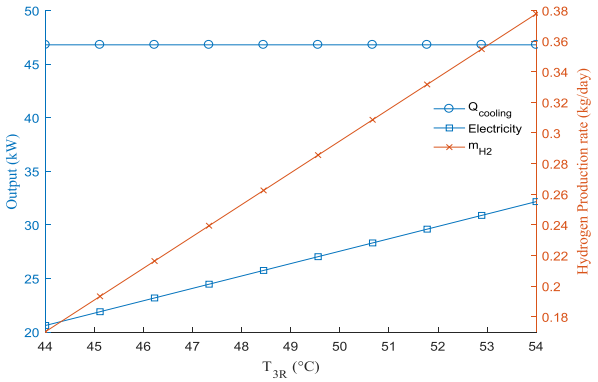

Fig. 9. Effect of varying the inlet temperature of the ORC's turbine on cooling capacity, electrical energy and the rate of hydrogen generation.

Performance of the system depends on solar irradiation intensity and the system's demand for complementary heating. Therefore, irradiation intensity is selected as one of the decision variables. Fig. 10 shows the effect of irradiation intensity on cooling capacity, electricity generation and exergy efficiency. As Fig. 10 declares, increase of irradiation intensity decreases exergy efficiency. It can be stated that when intensity of solar irradiation increases, more heat is provided for the system, which would decline exergy efficiency of the system. In other words, when irradiation intensity increases, more exergy is entered into the system and, as a consequence, exergy efficiency decreases. On the other hand, irradiation intensity does not have any significant effect on electricity generation since the other parameters are fixed.

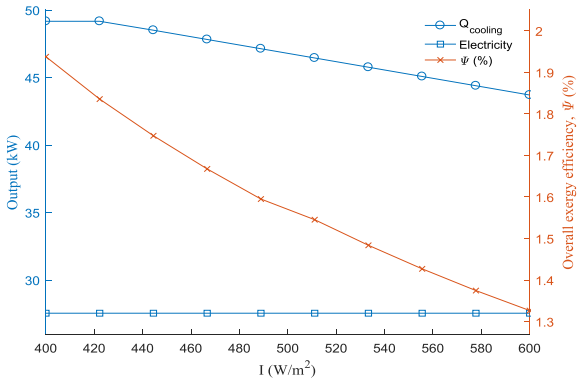

Fig. 10. Changes in exergy efficiency, cooling capacity and net energy generation by the ORC with variation of irradiation intensity.

Fig. 11 displays that the total exergy efficiency of the system reduces with increase of the collector's surface area. It means that efficiency and the collector's surface area are inversely related to each other. In the meantime, increase of the collector's area elevates the

[DOR: 20.1001.1.20089813.1398.6.1.6.6]

total cost rate of the system, noticeably. Therefore, it can be concluded that the collector contributes to the cost of the system, greatly. Therefore, increase of the collector's surface area burdens additional costs to the system, in addition to decreasing its efficiency.

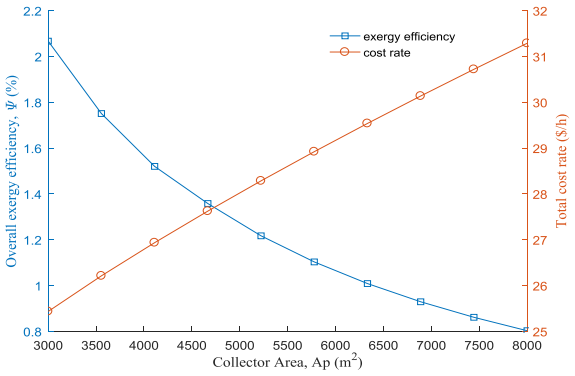

Fig. 11. Effect of the collector's surface area on the objective functions.

The effect of extending the surface area of the collector on the system outputs is depicted in Fig. 12. The results illustrate that surface extension decreases cooling capacity of the chiller and increases exergy loss meanwhile it does not alter electricity generation.

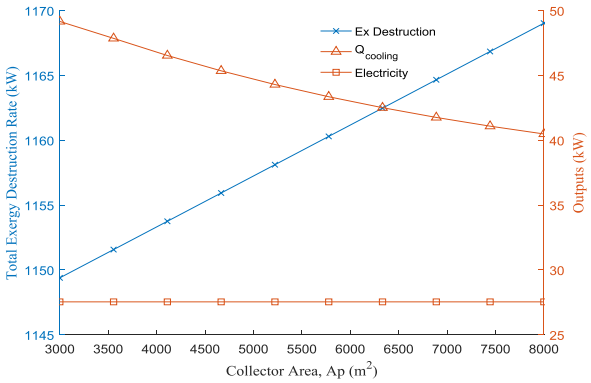

Fig. 12. The changes in total exergy loss, cooling capacity and net energy generation by the ORC with variations of the collector's surface area.

One of the other key design parameters of the system is inlet temperature of the ORC's evaporator (T_{3s}). The effect of this variable on exergy efficiency and total cost rate of the system is shown in Fig. 13. Based on this figure, increasing T_{3s} from 55 to 62.8 °C reduces exergy efficiency of the system considerably while the efficiency is constant at higher temperatures. Also, it can be observed that the total cost rate of the system increases with T_{3s}.

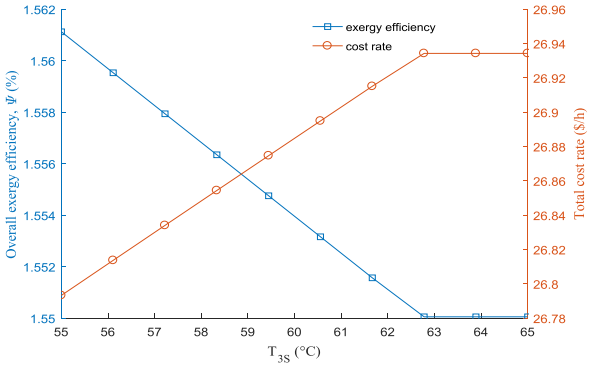

Fig. 13. Effect of the inlet temperature of the ORC's evaporator (T_{3s}) on the objective functions.

The effect of T_{3s} on cooling capacity, electricity generation and the rate of hydrogen production are depicted in Fig. 14. It can be seen that increase of T_{3s} does not alter the rates of hydrogen and electricity generation while it improves cooling capacity to some extent.

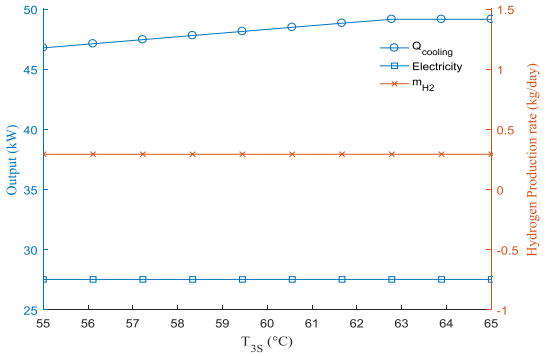

Fig. 14. Effect of the inlet temperature of the ORC's evaporator on cooling capacity, net energy generation by the ORC and rate of hydrogen production.

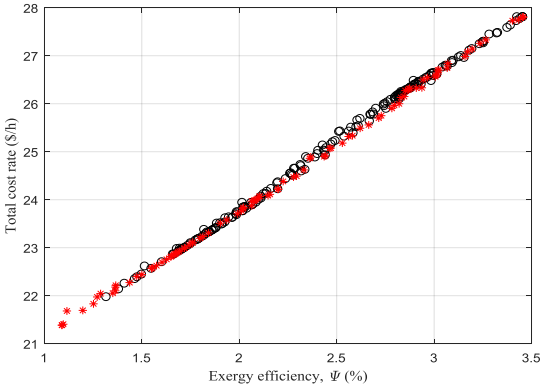

Fig. 15. Pareto chart of the two objective functions with respect to the decision variables.

Investigation of the results indicates that there is a paradox between the two defined objective functions and the design parameters. Existence of such paradox

[DOR: 20.1001.1.20089813.1398.6.1.6.6]

is essential for MOO. The Pareto chart of the two objective functions and a spectrum of changes for each decision variable is presented in Fig. 15. As it is clear, increase of the system's efficiency is accompanied with increase of the final costs. The first point on the Pareto curve determines the optimum status of total cost by neglecting exergy efficiency as an objective function. In addition, the last Pareto point refers to the optimum exergy efficiency of the system when it is the only objective function. It is also evident that both functions cannot remain at their best statuses, simultaneously. Therefore, the optimum point should lie where both functions are at their best statuses. Fig. 11 implies that the ideal point with such properties is not located on the Pareto curve. Though all points of the Pareto curve are the optimum results, the Pareto point that is located at the shortest distance from the ideal point can be considered as an optimum solution. MOO can identify this point. According to the MOO results, exergy efficiency and cost rate of the system vary between 1.0 to 3.5% and 21 to 28 $/h, respectively .In order to gain more insights about the impacts of the design parameters on the performance of the system, distribution of the decision variables is exhibited in Fig. 16. As Fig. 16a implies, the inlet temperature of the ORC's turbine is maximum at the optimum point. In the meanwhile, Fig. 16c states that the surface area of the collector is minimum at this state due to the high cost of the collector. The distribution of values in Fig. 16d declares that the optimum value of the collector's water mass flow rate is associated with an inter-correlation between the two objective functions.

5. Conclusion

The present study aims to perform the economic and thermodynamic analysis of a solar energy based integrated hybrid system through an optimization process leading to hydrogen production. Therefore, a dual-objective optimization through multi-objective particle warm algorithm is conducted to minimize the total cost of the system and maximize its efficiency. Furthermore, to evaluate the effect of important variables on performance of the system, a parametric study is performed. According to the optimum results, the system can provide the conditions of hydrogen generation with an acceptable efficiency. The following results were obtained and considered as the most important findings of this research:

- Parametric analysis of the system shows that the considered range of water mass flow rate of the collector can enhance efficiency of the system from 1.1 to 2.1%.
- The results indicated that increasing water mass flow rate of the collector in the determined range can enhance the rate of hydrogen production from 0.18 to 0.48 kg/s.
- The results demonstrated that increasing the maximum temperature of the organic Rankine cycle in the defined range can increase the rate of hydrogen generation from 0.18 to 0.38 kg/day. Growth of the inlet temperature of the turbine results in increasing the cost rate and exergy efficiency, simultaneously. However, its impact on increasing cost rate is more significant.
- The results revealed that surface area of the collector has a considerable effect on total cost. It means that, the total cost of the system increases with the collector area and the collector contributes to the costs, noticeably. Also, surface area of the collector has a negative impact on exergy efficiency.
- Multi-objective optimization of the system revealed that exergy efficiency of the system can increase up to 3.5%. Furthermore, if the total cost of the system be considered as the only objective function, then total cost rate can decrease to 21 $/h.

By considering the both objective functions of exergy efficiency and total cost, the optimization algorithm was executed 10 times and the average results were presented. In this respect, total cost and exergy efficiency were determined as 21.9462 $/h and 2.2712%, respectively. The corresponding point has the shortest distance from the ideal point. To promote performance of the proposed system, one of the most useful solutions is employing two renewable energy resources, simultaneously. The two energy resources can be selected according to the environmental conditions of some regions that

[DOR: 20.1001.1.20089813.1398.6.1.6.6]

have access to renewable sources of energy.

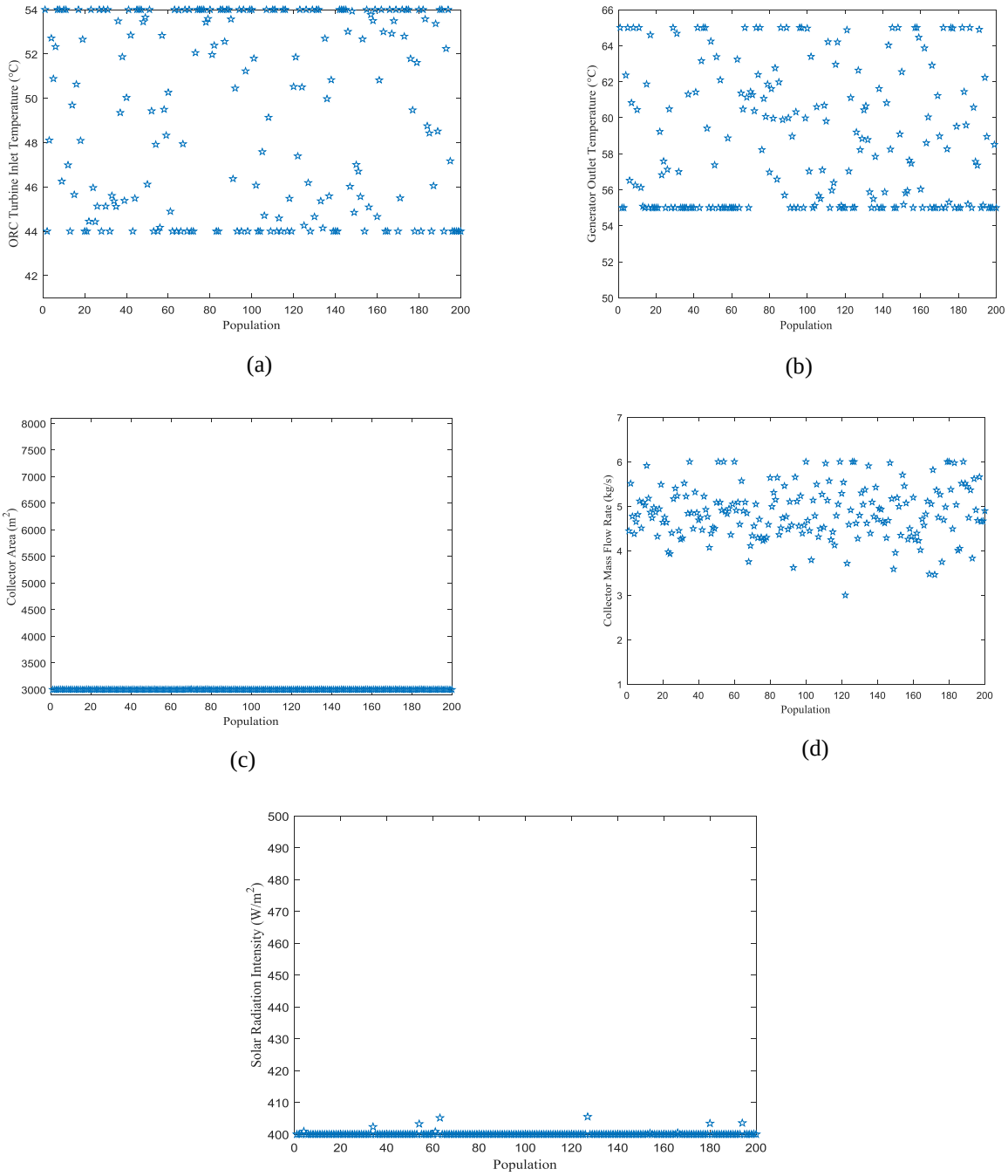

Fig. 16. Distribution of the decision variables on the boundary of the Pareto curve; a) inlet temperature of the ORC's turbine, b) inlet temperature of the generator, c) collector area, d) water mass flow rate of the collector, and e) irradiation intensity

[DOR: 20.1001.1.20089813.1398.6.1.6.6]

Nomenclature/ Abbreviations

A_p	Surface area, m^2
$\dot{C}$	Cost rate, \$/h
C_p	Specific heat capacity
Ex	Exergy
$\dot{E}x$	kw, exergy rate
F_R	Heat loss factor
F'	Collector efficiency factor
G	Generator
H	Enthalpy, kJ/kg
I	Irradiation intensity
$\dot{m}_{col}$	Collector's water mass flow rate
Q_u	Collector's outlet heat
Q_L	Collector's heat loss
U_l	Coefficient of the collector's total loss
X	Weight percentage of Li-Br
Z	\$Equipment purchase cost
$\dot{Z}$	Cost rate, \$/h
Subscript indices	
Col	Collector
Cond	Condenser
Ev	Evaporator
In	Inlet
Is	Isentropic
L	Loss
Out	Outlet
P	Pump
R	Organic Rankine Cycle
S	Sun
Tur	Turbine
U	Utilized
∘	Standard conditions
Greek letters	
α	Absorption coefficient
φ	The factor of performance and maintenance
η	Efficiency
$\eta_\circ$	Visual efficiency
τ	Transport
$(\alpha\tau)$	Transmission coefficient of the effective product
Ψ	Exergy efficiency
Abbreviations	
ORC	Organic Rankine Cycle
PEM	Proton Exchange Membrane
CRF	capital recovery factor
FPSCs	flat plate solar collectors

References

[1] Ahmadi, P., Dincer, I., Rosen M. A.,2013. Energy and exergy analyses of hydrogen production via solar-boosted ocean thermal energy conversion and PEM electrolysis. Int J Hydrogen Energy, 38(4):1795e805.

[2] Bicer, Y., Dincer, I., 2016. Development of a new solar and geothermal based combined system for hydrogen production. Solar Energy 127, 269–284**.**

[3] Ahmadi, P., Dincer, I., Rosen, M. A., 2014. Multi-objective optimization of a novel solar-based multigeneration energy system. Solar Energy, Vol. 108, pp. 576-591.

[4] Joshi, A. S., Dincer, I., Reddy B. V., 2016. Effects of various parameters on energy and exergy efficiencies of a solar thermal hydrogen production system. internationaljournal of hydrogen energy I-11.

[5] Yuksel, Y. E., Ozturk, M., 2016. Thermodynamic and thermoeconomic analyses of a geothermal energy based integrated system for hydrogen production. internationaljournal of hydrogen energy I-17.

[6] Ahmadi, P., Dincer, I., Rosen, M. A., 2014. Multi-objective optimization of an ocean thermal energy conversion system for hydrogen production. internationaljournal of hydrogen energy I-8.

[7] Ahmadi, P., Dincer, I., Rosen, M. A., 2014. Multi-objective optimization of a novel solar-based multigeneration energy system. Solar Energy 108, 576–591.

[8] Dincer, I., Zamfirescu, C., 2012. Renewable-energy-based multigeneration systems. Int. J. Energy Res. 46 (15), 1403–1415.

[9] Ozturk, M., Dincer, I., 2012. Thermodynamic analysis of a solar-based multi-generation system with hydrogen production. Appl. Therm. Eng. 51 (1), 1235–1244.

[10] Al-Sulaiman, F. A., Dincer, I., Hamdullahpur, F., 2013. Thermoeconomic optimization of three generation using organic Rankine cycle: Applications. Energy Conversion and Management Vol. 69, No. 4, pp. 209-216.

[11] Yilmaz, C., Kanoglu,M., Bolatturk, A., Gadalla, M., 2012. Economics of hydrogen production and liquefaction by geothermal energy, International

[DOR: 20.1001.1.20089813.1398.6.1.6.6]

Journal of Hydrogen Energy, Vol. 37, No. 2, pp. 2058-2069.
[12] Ouali, S., Chader, S., Belhamel, M., Benziada, M., 2011. The exploitation of hydrogen sulfide for hydrogen production in geothermal areas, International Journal of Hydrogen Energy, Vol. 36, No. 6, pp. 4103-4109.
[13] Yuksel, Y. E., Ozturk, M., Dincer, I., 2016. Thermodynamic performance assessment of a novel environmentally-benign solar energy based integrated system. Energy Conversion and Management, Vol. 119, pp. 109-120.
[14] Farahat, S, Sarhaddi, F, Ajam, H. , Exergetic optimization of flat plate solar collectors. Renew Energy 2009;34(4):1169e74.
[15] Khanmohammadi, S., Atashkari, K., Kouhikamali, R. ,2015. Exergoeconomic multi-objective optimization of an externally fired gas turbine integrated with a biomass gasifier. Appl Therm Eng 91:848e59.
[16] Khanmohammadi, S., Azimian, A. R.,2013. Exergoeconomic evaluation of a two-pressure level fired combined-cycle power plant. J Energy Eng 141(3).
[17] Palacios-Bereche, R., Gonzales, R., Nebra, S. A.,2012. Exergy calculation of lithium bromideewater solution and its application in the exergetic evaluation of absorption refrigeration systems LiBr-H2O. Int J Energy Res, 36(2):166e81.
[18] Kotas, T. J.,1995. The exergy method of thermal plant analysis. Krieger Melbourne, FL.
[19] Khanmohammadi, S., Azimian A. R., Khanmohammadi S., 2013. Exergy and exergoeeconomic evaluation of Isfahan steam power plant. Int J Exergy 12(2):249e72.
[20] Bejan, A., Moran, M. J.,1996 Thermal design and optimization. John Wiley & Sons.
[21] Ameri, M., Ahmadi, P.,2008. Khanmohammadi S. Exergy analysis of a 420 MW combined cycle power plant. Int J Energy Res 32(2):175e83.
[22] Ozlu, S.,2015. Development and analysis of solar energy based multigeneration systems. University of Ontario Institute of Technology.
[23] Genc, G. C¸ elik, M., Genc¸ M. S., 2012. Cost analysis of wind-electrolyzerfuel cell system for energy demand in Pınarbas¸ı-Kayseri. Int J Hydrogen Energy 37(17):12158e66.
[24] Peters, M. S, Timmerhaus, K., West R. E.,1968. Plant design and economics for chemical engineers, vol. 4. New York: McGraw-Hill.
[25] Balli, O, Aras, H, Hepbasli, A., 2008. Exergoeconomic analysis of a combined heat and power (CHP) system. Int J Energy Res 32(4):273e89.
[26] Ma, L., Lu, Z., Zhang, J., Liang, I., 2010. Thermal performance analysis of the glass evacuated tube solar collector with U-tube. Building and Environment. 45 1959e1967.
[27] Khanmohammadi, S., Heidarnejad, P., Javani, N., Ganjehsarabi, H., 2017. Exergoeconomic analysis and multi objective optimization of a solar based integrated energy system for hydrogen production. international journal of hydrogen energy xxx 1e11.
[28] Khanmohammadi, S., Ahmadi, P., Atashkari, K., 2015. Kouhikamali R. Design and optimization of an integrated system to recover energy from a gas pressure reduction station. Progress in clean energy. volume 1: analysis and modeling. p. 89.
[29] Kim, D. S., Infante Ferreira, C. A, 2006. A Gibbs energy equation for LiBr aqueous solutions. International Journal of Refrigeration 29, 36–46.
[30] Bejan, A., Kearney, D., Kreith, F., 1981. Second law analysis and synthesis of solar collector systems. J Sol Energy Eng,103(1):23e8.

[DOR: 20.1001.1.20089813.1398.6.1.6.6]